ACS OMEGA

Article

Cite This: ACS Omega 2019, 4, 16517−16523

http://pubs.acs.org/journal/acsodf

CLG from Hemp Seed Inhibits LPS-Stimulated Neuroinflammation in BV2 Microglia by Regulating NF-κB and Nrf-2 Pathways

Shanshan Wang,[§] Qian Luo,[§] Yuefang Zhou, and Peihong Fan*

Department of Natural Product Chemistry, Key Laboratory of Chemical Biology (Ministry of Education), School of Pharmaceutical Sciences, Shandong University, Jinan 250012, China

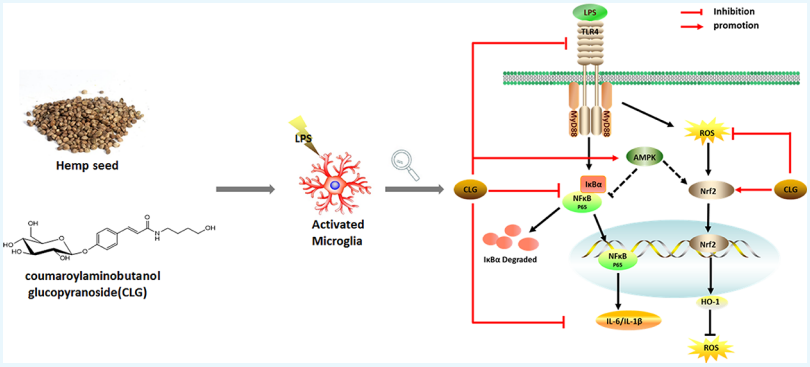

ABSTRACT: The healthy benefits of hemp (*Cannabis sativa* L.) seed have often been attributed to its oils and proteins. Recent studies reveal that hemp seed phenylpropionamides could also show various bioactivities. Continuation of our study on hemp seed provided a phenylpropionamide, coumaroylaminobutanol glucopyranoside (CLG). This work investigated the neuroprotective effect of CLG and its underlying mechanism using lipopolysaccharide-induced BV2 microglia. Our study demonstrated that CLG increased adenosine monophosphate-activated protein kinase (AMPK) expression, suppressed the nuclear factor-kappa B (NF-κB) signaling pathway by inhibiting the phosphorylation of IκBα and NF-κB p65 and decreased proinflammatory cytokine levels in a concentration-dependent manner. Furthermore, CLG reduced the production of cellular reactive oxygen species and stimulated the nuclear factor erythroid 2-related factor 2 (Nrf-2) signaling pathway. Collectively, these results suggested that CLG effectively and simultaneously inhibited inflammatory responses and oxidative stress through the NF-κB and Nrf-2 signaling pathways. AMPK was also involved in the anti-inflammatory effect of CLG. This study provides new insights into the diverse bioactive constituents of hemp seed.

1. INTRODUCTION

As the major resident neuroimmune cells, microglia cells have a pivotal role in the pathology of neurodegenerative diseases.[1] In response to external pathogenic infections or cell debris, microglia cells are activated quickly and release neurotrophic factors, performing their host-defense function. However, persistent microglia activation will produce excessive amounts of various proinflammatory mediators, such as interleukin-1β (IL-1β), IL-6, and tumor necrosis factor-α (TNF-α), reactive oxygen species (ROS), and nitric oxide (NO), which contribute to neurodegenerative processes and result in neuronal injury.[2] Therefore, pharmaceuticals that can provide inhibitory effects on microglia overactivation are considered as an effective strategy to control neurodegenerative progression.

Hemp (*Cannabis sativa* L.) seed has been used as food and traditional medicine for centuries.[3] Hemp seed extracts, containing lignanamides and other phenylpropionamides, showed potential anti-inflammatory[4,5] and antioxidative[6] capacity and improved impaired learning and memory induced by chemical drugs in mice.[7,8] Our previous study isolated coumaroylaminobutanol glucopyranoside (CLG, Figure 1a) from the hemp seed, a phenylpropionamide compound, which showed significant activity in the antineuroinflammatory screening test using a lipopolysaccharide (LPS)-induced BV2 microglia model.[4] In the current work, we aimed to understand how CLG could inhibit LPS-stimulated neuroinflammation in BV2 microglia.

Toll-like receptor 4 (TLR4), a well-known transmembrane receptor, is able to specifically recognize LPS in microglia signaling.[9] Upon stimulation, activated TLR4 recruits the downstream adaptor myeloid differentiation primary response gene 88 (MyD88) to activate the nuclear factor-kappa B (NF-κB) pathway, which regulates the expression of various proinflammatory mediators.[10] Furthermore, it is now widely accepted that LPS-induced inflammation can elevate cellular ROS levels in microglia, and high levels of ROS may in return contribute to the release of various NF-κB-mediated proinflammatory mediators.[11] As an important defense system, nuclear factor erythroid 2-related factor 2 (Nrf-2), one of the major redox-sensitive transcription factors, can be activated by

Received: July 13, 2019
Accepted: September 12, 2019
Published: September 26, 2019

DOI: 10.1021/acsomega.9b02168
ACS Omega 2019, 4, 16517−16523

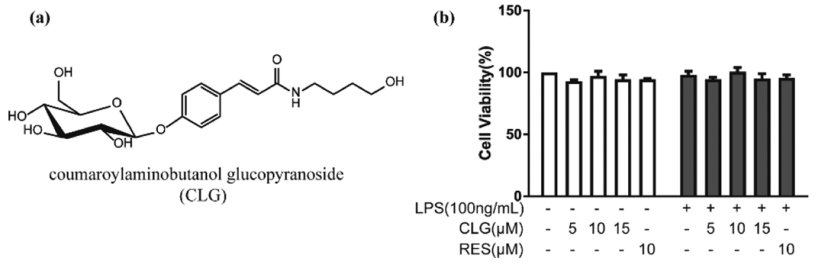

Figure 1. Effect of CLG on the cell viability of BV2 microglia with or without LPS stimulation. (a) Structure of CLG. (b) BV2 cells were cotreated with various concentrations of CLG (5, 10, 15 μM) or RES (10 μM) with or without LPS (100 ng/mL) for 24 h. Cell viability was determined by the MTT assay. (The data are expressed as the mean ± SD of three experiments.)

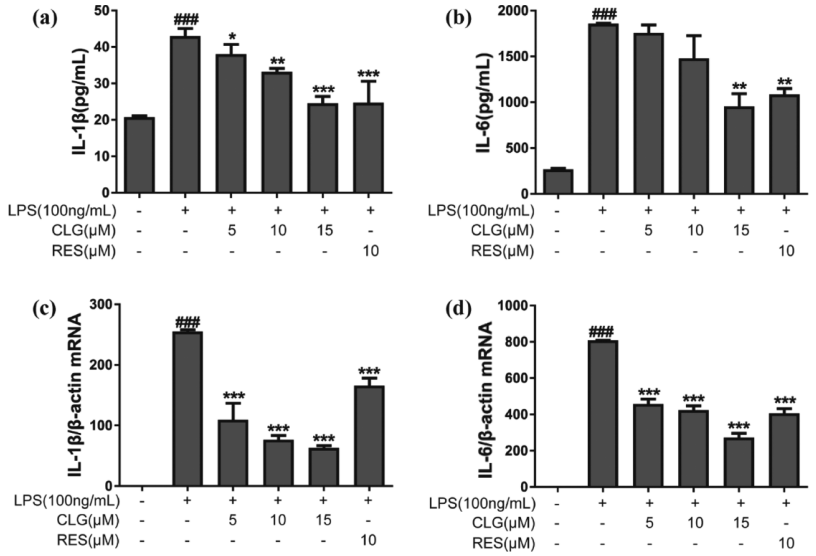

Figure 2. CLG reduced proinflammatory cytokine production in LPS-stimulated BV2 microglia. BV2 cells were pretreated with 5, 10, and 15 μM CLG for 1 h and then stimulated with LPS (100 ng/mL). After coincubation for 24 h, the supernatants were collected for the measurement of IL-1β (a) and IL-6 (b) by ELISA. After coincubation for 6 h, total RNA was isolated, and relative IL-1β (c) and IL-6 (d) mRNA expression was measured by RT-PCR. (Data are presented as the mean ± SD from at least three independent experiments. *p < 0.05, **p < 0.01, and ***p < 0.001 compared with the LPS-treated group; $^{\#\#\#}p$ < 0.001 compared with the control group.)

oxidative stress, leading to the expression of hemeoxygenase-1 (HO-1) and other antioxidant enzymes. Adenosine monophosphate-activated protein kinase (AMPK), a key regulator of cellular energy homeostasis, also plays an evident role in regulating oxidative stress and neuroinflammation in LPS-treated microglia.[12] AMPK activation could inhibit the inflammatory responses induced by the NF-κB system[13] and could prevent neuronal oxidative stress. There is cross talk between the AMPK and Nrf2/ARE pathways.[12]

Here, we evaluated the neuroprotective effect of CLG and investigated the underlying molecular mechanisms involving TLR4/NF-κB and Nrf-2/HO-1 pathways and the possible role of AMPK in BV2 microglia.

2. RESULTS AND DISCUSSION

Activated microglia can respond quickly to various stimuli, and LPS is one of the most frequently used stimuli in different inflammatory models in vitro and in vivo.[14,15] Therefore, we used LPS-stimulated BV2 microglia as an in vitro inflammatory model.

2.1. Effect of CLG on the Viability of BV2 Microglia. The cytotoxic effect of CLG was determined using a 3-(4,5-dimethylthiazol-2-yl)-2,5-diphenyl-tetrazolium bromide (MTT) assay. Compared with the vehicle control, treatment with various concentrations of CLG (5, 10, 15 μM) or RES (resveratrol, 10 μM) had no significant effect on cell survival (Figure 1b). Moreover, LPS (100 ng/mL) combined with CLG or RES did not affect the viability of BV2 cells. Thus, 5, 10, and 15 μM were selected for CLG as the treatment concentrations for further analysis, RES (10 μM) was used as a positive control, and LPS (100 ng/mL) was used as a stimulus in this study.

2.2. Effect of CLG on Proinflammatory Cytokine Production in LPS-Induced BV2 Microglia. Proinflammatory cytokines are involved in the pathogenesis of neuroinflammation and multiple neurodegenerative diseases.[2] To evaluate the effects of CLG on proinflammatory cytokine production, IL-1β and IL-6 levels were determined by the enzyme-linked immunosorbent assay (ELISA). Figure 2a,b shows that LPS stimulation increased the secretion of proinflammatory cytokines significantly, whereas CLG prevented this effect and significantly decreased IL-1β and IL-6 levels in a dose-dependent manner compared with the LPS group. To further evaluate CLG's effect on mRNA levels of IL-1β and IL-6, a reverse transcription polymerase chain reaction (RT-PCR) experiment was performed. Pretreatment with CLG reduced IL-1β (Figure 2c) and IL-6 (Figure 2d) mRNA

DOI: 10.1021/acsomega.9b02168
ACS Omega 2019, 4, 16517−16523

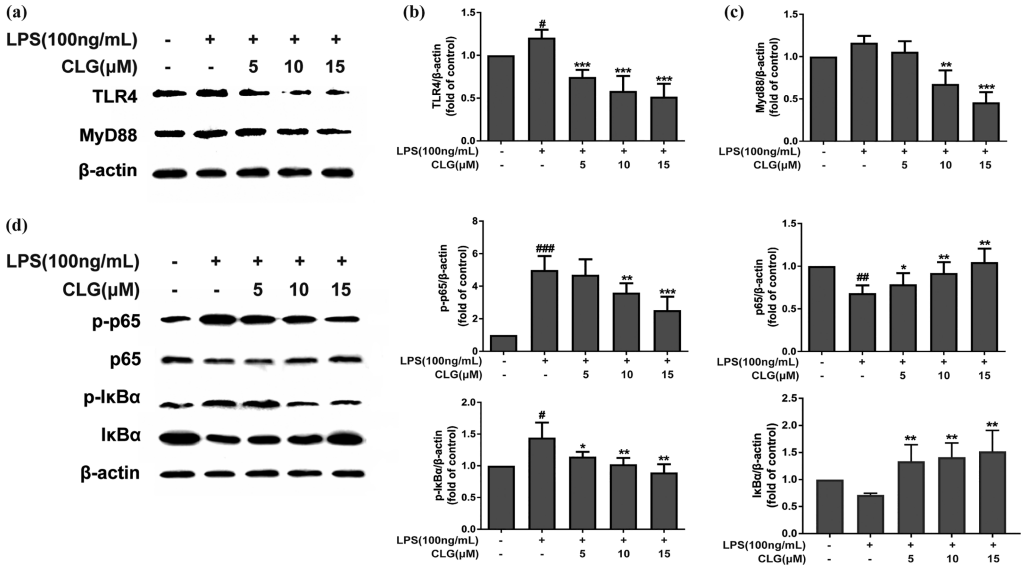

Figure 3. CLG inhibited TLR4/NF-κB protein expression in LPS-induced BV2 microglia. BV2 cells were pretreated with CLG for 1 h and stimulated with LPS. After stimulation for 24 h, cell extracts were prepared and subjected to western blotting with TLR4 and MyD88 antibodies. After stimulation for 1 h, cell extracts were prepared and subjected to western blotting with IκBα, phospho-IκBα, NF-κB p65, and phospho-NF-κB p65 antibodies. β-Actin was used as the internal control for normalization. (a) Western blot bands of TLR4 and MyD88. (b) The density of TLR4 bands was measured, and their ratio was calculated. (c) Density ratio of MyD88 bands. (d) Western blot bands of IκBα, phospho-IκBα, NF-κB p65, and phospho-NF-κB p65. (e−h) Density ratio of phospho-NF-κB p65, p65, phospho-IκBα, and IκBα. (The results are presented as the mean ± SD from at least three independent experiments. $^{*}p < 0.05$, $^{**}p < 0.01$, and $^{***}p < 0.001$ compared with cells treated with LPS; $^{\#}p < 0.05$, $^{\#\#}p < 0.01$, and $^{\#\#\#}p < 0.001$ compared with the control.)

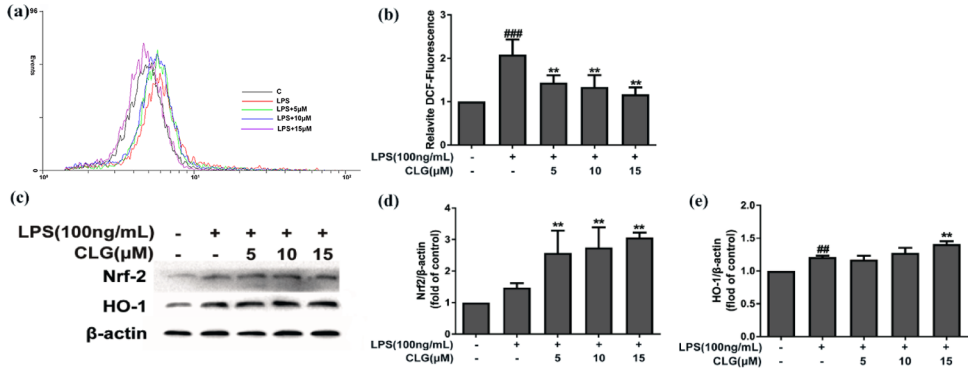

Figure 4. CLG reduced cellular ROS generation and promoted Nrf-2/HO-1 expression in LPS-induced BV2 microglia. BV2 cells were treated with CLG for 1 h prior to LPS stimulation for 24 h. (a) Cellular ROS levels were measured using DCFH-DA by flow cytometry. (b) Quantification of the relative % of cells with ROS production. (c) Cell lysates were collected and analyzed using western blotting for Nrf-2 and HO-1. (d,e) The density of Nrf-2 and HO-1 bands was measured, and their ratio was calculated. β-Actin was used as the internal control for normalization. (The results are presented as the mean ± SD from at least three independent experiments. $^{**}p < 0.01$ compared with cells treated with LPS; $^{\#\#}p < 0.01$ and $^{\#\#\#}p < 0.001$ compared with the control.)

expression significantly in a concentration-dependent manner compared to the LPS group.

2.3. Effect of CLG on TLR4/NF-κB Expression in LPS-Induced BV2 Microglia. TLR4 is a starting point in the entire LPS-initiated signaling pathway, and LPS is recognized by TLR4.[16] TLR4 undergoes dimerization and recruits its downstream adaptors including MyD88. The MyD88-dependent pathway triggers a signaling cascade, leading to NF-κB pathway activation and then the production of proinflammatory cytokines.[17] TLR4/NF-κB signaling is one of the major pathways mediating immune and inflammatory responses and is closely involved in the expression of inflammatory mediators.[17]

The effects of CLG on TLR4/NF-κB signaling were detected in this study. Western blotting showed that LPS increased TLR4 expression significantly, compared to the control group, but CLG treatment significantly inhibited the LPS-induced increase of TLR4 dose-dependently (Figure 3a,b). MyD88 is a downstream adaptor for TLR4 and triggers a signaling cascade, leading to NF-κB activation, so we further checked the MyD88-dependent mechanism. Figure 3a,c demonstrates that CLG could suppress the LPS-induced activation of MyD88, indicating that CLG could interfere in LPS-induced inflammation through a MyD88-dependent manner.

The NF-κB pathway plays a crucial role in the activation of inflammatory responses and the regulation of inflammatory cytokine production.[18] Phosphorylation and degradation of IκB are primarily involved in NF-κB activation triggered by LPS, and we explored the effect of CLG on the activation of

DOI: 10.1021/acsomega.9b02168
ACS Omega 2019, 4, 16517−16523

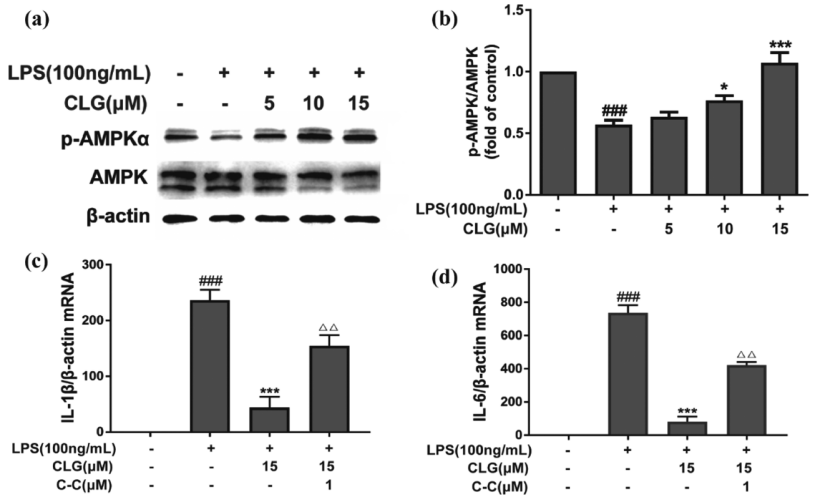

Figure 5. CLG increased AMPK activation in LPS-induced BV2 microglia. BV2 cells were treated with CLG for 1 h prior to LPS stimulation for 24 h. Cell lysates were collected and analyzed using western blotting for phospho-AMPK and AMPK (a). The density of phospho-AMPK and AMPK bands was measured, and their ratio was calculated (b). Cells were pretreated with or without CLG and C−C (1 μM) for 1 h and then coincubated with LPS for 6 h, total RNA was isolated, and relative IL-1β (c) and IL-6 (d) mRNA expression was measured by RT-PCR. β-Actin was used as the internal control. (The results are presented as the mean ± SD from at least three independent experiments. *p < 0.05 and ***p < 0.001 compared with cells treated with LPS; $^{\#\#\#}p$ < 0.001 compared with the control.)

NF-κB p65 and IκBα. Results (Figure 3d) revealed that LPS treatment increased the phosphorylation of NF-κB p65 and IκBα but decreased the expression of IκBα and NF-κB p65 compared with the vehicle control. However, CLG dose-dependently reduced NF-κB p65 and IκB phosphorylation levels and promoted NF-κB 65 and IκB expression compared with the LPS treatment group (Figure 3d−h), indicating that CLG could prevent LPS-induced inflammation through inhibiting the activation of the NF-κB pathway.

Taken together, these results supported that the TLR4/MyD88/NF-κB pathway was involved in the effect of CLG on protecting BV2 cells against LPS-induced neuroinflammation.

2.4. Effect of CLG on Cellular ROS Production and Nrf-2/HO-1 Expression in LPS-Induced BV2 Microglia. LPS treatment dramatically increases not only proinflammatory cytokine production but also ROS levels in microglia.[19] ROS is a hallmark of inflammatory responses and oxidative damage in microglia.[20] Here, we investigated the antioxidant effect of CLG on ROS generation in LPS-induced BV2 cells by dichlorodihydrofluorescein diacetate (DCFH-DA). As expected, CLG treatment dose-dependently quenched ROS production compared with the LPS-treated group (Figure 4a,b), suggesting that CLG alleviated oxidative damage by decreasing the production of ROS in LPS-activated microglia.

As an important cellular defense mechanism, Nrf-2-mediated signaling has been shown to be vital in modulating redox homeostasis and attenuating oxidative stress in neurodegenerative diseases.[21] Nrf-2 can be rapidly upregulated by various oxidative stress stimuli, including LPS and ROS, and can then regulate inflammatory and antioxidant responses. As one of the downstream antioxidant genes of Nrf-2, HO-1 has been recently demonstrated to exhibit important immunomodulatory and anti-inflammatory functions.[22] Therefore, the regulation of the Nrf-2/HO-1 pathway can benefit the treatment of inflammation-related diseases. This pathway can be activated not only by various cellular stresses but also by chemical inducers from exogenous sources. Many small molecule Nrf-2 inducers from natural sources have been reported.[23]

To better understand the antioxidant molecular pathway of CLG, we further explored whether the Nrf2/HO-1 signaling is affected by CLG using western blot analysis. As shown in Figure 4c−e, Nrf2/HO-1 was slightly activated in the LPS stimulated group, possibly attributed to the oxidative stress induced by LPS. Pretreatment with CLG significantly upregulated Nrf-2 (Figure 4c,d) and HO-1 (Figure 4c,e) protein expression dose-dependently, suggesting that CLG was a Nrf-2 inducer, and the activation of Nrf-2/HO-1 could contribute to the antioxidative effect of CLG.

These results show that CLG could inhibit neuroinflammation partly via antioxidant mechanisms by decreasing ROS production directly and activating Nrf-2/HO-1 in LPS-induced BV2 microglia.

2.5. Effect of CLG on AMPK Activation in LPS-Induced BV2 Microglia. AMPK has attracted increasing attention not only for its crucial regulation of energy metabolism homeostasis but also for the correlation between antioxidant and anti-inflammation in neurodegenerative diseases.[24] Emerging evidence shows that AMPK activation contributes to the antioxidant and anti-inflammatory mechanisms by enhancing Nrf-2/HO-1 signaling and inhibiting NF-κB signaling.[12,13] Previous studies have revealed that AMPK participates in regulating the release of IL-1β, IL-6, TNF-α, and ROS generation.[25,26] Considering the critical role of AMPK in inflammatory responses and oxidative stress, we detected AMPK activation in LPS-induced BV2 microglia by western blotting. As expected, compared with the LPS group, CLG reversed the effect of LPS on the expression of phosphorylated AMPK dose-dependently (Figure 5a,b). To check if the impact on AMPK is related to CLG's anti-inflammatory effect, further investigation of AMPK was carried out by adding an inhibitor, dorsomorphin (compound C, C−C), and the expression of IL-6 and IL-1β mRNA was measured using RT-PCR. The inhibitor counteracted the CLG effect on the mRNA levels of proinflammatory cytokines (IL-1β, IL-6) (Figure 5c,d) in LPS-induced BV2 microglia, indicating that the inhibitory effects of CLG on LPS-induced neuroinflammatory responses were closely linked with AMPK activation. On the basis of the

DOI: 10.1021/acsomega.9b02168
ACS Omega 2019, 4, 16517−16523

reported AMPK/NF-κB pathway,[12,13] we propose that the CLG effect on the NF-κB pathway is related to AMPK, but further work still needs to be designed to reveal the effect of CLG on signals between the AMPK and NF-κB pathways. The NF-κB subunits are not direct phosphorylation targets of AMPK, but several downstream targets of AMPK, such as SIRT1 (silent information regulator), p53, peroxisome proliferator-activated receptor γ co-activator 1α (PGC-1α), and Forkhead box O (FoxO) factors, could mediate the inhibition of NF-κB signaling.[13] The effects of CLG on these downstream targets of AMPK should be explored in future to understand the effect of CLG on the cross talk between the AMPK and NF-κB pathways. Besides, the inhibitor of AMPK only partially restored the IL-1β and IL-6 mRNA expression; other factors not involved in our study such as PI3K/AKT, MAPK, ERK, and JNK may also be involved in LPS-induced proinflammatory cytokine expression.[27,28] More mechanism study needs to be implemented to better understand the effect of CLG in LPS-stimulated microglia.

3. CONCLUSIONS

In conclusion, this study demonstrated for the first time that CLG could inhibit LPS-induced neuroinflammation and oxidative stress in BV2 microglia through the TLR4/NF-κB and Nrf-2/HO-1 signaling pathways. Moreover, AMPK also played an important role in the anti-inflammatory effect of CLG. However, this work only demonstrated that CLG treatment had a close connection with AMPK, TLR4/NF-κB, and Nrf-2/HO-1 signaling pathways. To determine the direct target of CLG in microglia, more studies are still needed. Our findings contribute to the knowledge of diverse bioactive compounds from hemp seed and the potential of hemp seed in the treatment of microglia-related neuroinflammatory diseases.

4. EXPERIMENTAL METHODS

4.1. Reagents and Antibodies. LPS (*Escherichia coli* 0111:B4) and 2′,7′-DCFH-DA were from Sigma-Aldrich (St Louis, MO, USA). Penicillin and streptomycin, 0.05% (w/v) trypsin/ethylenediaminetetraacetic acid, and Dulbecco's modified Eagle's medium (DMEM) were purchased from Macgene (Beijing, China). Fetal bovine serum (FBS) was obtained from Biological Industries (Kibbutz Beit Haemek, Israel). RES, MTT, and dimethyl sulfoxide (DMSO) were purchased from Solarbio (Beijing, China). Dorsomorphin (compound C, C−C) was purchased from Aladdin (Shanghai, China). ELISA kits specific for mouse IL-1β and IL-6 were purchased from Boster (Wuhan, China). RIPA lysis buffer and BCA protein kit were purchased from Beyotime (Shanghai, China). Immobilon western chemiluminescent HRP substrate (ECL) was obtained from Millipore (Billerica, MA, USA). TRIzol reagent, PrimeScript RT reagent kit, and SYBR Premix Ex Taq were obtained from Takara (Shiga, Japan), and RT-PCR primers were purchased from Sangon Biotech (Shanghai, China).

Antibodies against NF-κB p65 and Nrf-2 were obtained from Santa Cruz Biotechnology (CA, USA). Antibodies against IκBα, phospho-IκBα, and TLR4 were from Abcam (Cambridge, UK). Antibodies against AMPK were from ABclonal (Wuhan, China). Antibodies against MyD88, phospho-NF-κB p65, phospho-AMPKα, HO-1, and β-actin were obtained from Cell Signaling Technologies (MA, USA), and horseradish peroxidase (HRP)-conjugated secondary antibodies were obtained from ZSGB-BIO (Beijing, China).

4.2. Extraction of CLG. CLG was isolated from hemp seed as previously described,[4] and the chemical structure of CLG is illustrated in Figure 1a. The air-dried seeds (10.7 kg) were crushed and defatted with petroleum ether (2 times, 30 L for 60 h) and then extracted with 95% EtOH under reflux (3 times, 50 L for 2 h), and the filtrate was concentrated under vacuum to 500 mL. The EtOH extract (1 kg) was subsequently separated by an AB-8 macroporous adsorption resin column (elution with EtOH/H_2O), a Sephadex LH-20 column (elution with MeOH, 1.05 g), a medium-pressure reversed-phase column liquid chromatograph (elution with MeOH/H_2O, 690 mg), and a high-speed countercurrent chromatograph (elution with EtOAc/MeOH/H_2O). Successively, CLG (28.80 mg) was obtained, and high-performance liquid chromatography analysis provided a purity of more than 98%.

4.3. Cell Culture and Drug Treatment. A murine microglia cell line (BV2) was purchased from the Cell Bank of the Institute of Biochemistry and Cell Biology, Chinese Academy of Sciences (Shanghai, China). BV2 cells were maintained in DMEM supplemented with 10% (v/v) FBS and 1% penicillin and streptomycin at 37 °C in a humidified atmosphere containing 5% CO_2.

Prior to the experiments, cells were transferred to 96-well (8×10^3 cells/well), 12-well (3×10^4 cells/well), or 6-well (1×10^6 cells/well) plates and incubated overnight. In all experiments, BV2 cells were pretreated with either DMSO (vehicle control) or CLG (5, 10, 15 μM) for 1 h before the addition of LPS (100 ng/mL). RES (10 μM) was used as a positive control. CLG was dissolved in DMSO, stored at −20 °C, and diluted with the culture medium to obtain the desired final concentration before use. The final concentration of DMSO was always less than 0.4%. LPS was dissolved in sterilized phosphate-buffered saline (PBS) and stored at −20 °C and then diluted with the culture medium.

4.4. Measurement of Cell Viability. Cell viability was assessed by MTT. BV2 cells were plated into 96-well culture plates and incubated overnight and then incubated with various concentrations of CLG or RES for 1 h prior to treatment with LPS for another 24 h. The culture medium was removed, and 10 μL of MTT was added (0.5 mg/mL) and incubated for 4 h. The formazan crystals were dissolved in 100 μL of DMSO. Absorbance was read at 540 nm. The results are expressed as a percentage of control cells.

4.5. Measurement of Cytokines by ELISA. Proinflammatory cytokine production was assayed using ELISA kits according to the manufacturer's instructions. BV2 cells were treated with CLG in the absence or presence of LPS for 24 h. Culture supernatants were collected and centrifuged, and the levels of IL-1β and IL-6 were assessed. The optical density of each well was measured at 450 nm.

4.6. Measurement of Intracellular ROS. DCFH-DA, a stable nonpolar compound that diffuses readily into cells and yields DCFH, was used to detect cellular ROS generation. After drug treatment, cells were washed with ice-cold PBS and incubated with serum-free medium containing 10 μg/mL of DCFH-DA at 37 °C for 30 min in the dark. Thereafter, cells were washed with PBS and then harvested and resuspended in PBS. Fluorescence intensity of DCF fluorescence as the oxidized product of DCFH was analyzed with a 488 nm excitation filter and a 525 nm emission wavelength by flow cytometry (FACS Calibur, Becton Dickinson, Franklin Lakes, NJ).

DOI: 10.1021/acsomega.9b02168
ACS Omega 2019, 4, 16517−16523

4.7. RNA Extraction and RT-PCR. Total RNA was extracted using the TRIzol reagent, and RNA concentration was evaluated at 260 and 280 nm. RNA (1 μg) was reverse-transcribed into cDNA using the PrimeScript RT reagent kit. RT-PCR was carried out with cDNA and SYBR Premix Ex Taq. The RT-PCR conditions were 95 °C for 2 min, 40 cycles at 95 °C for 15 s, 53 °C for 15 s, and 72 °C for 20 s. The relative mRNA expression was normalized to β-actin expression and calculated by the $2^{-\Delta\Delta CT}$. The primer sequences are as follows: IL-1β (forward: 5′-CAT ATG AGC TGA AAG CTC TCC A-3′, reverse: 5′-GAC ACA GAT TCC ATG GTG AAG TC-3′); IL-6 (forward: 5′-CCA CTT CAC AAG TCG GAG GC-3′, reverse: 5′-CCA GCT TAT CTG TTA GGA GA-3′); and β-actin (forward: 5′-GTG ACG TTG ACA TCC GTA AAG A-3′, reverse: 5′-GCC GGA CTC ATC GTA CTC C-3′).

4.8. Western Blot Analysis. After drug treatment, BV2 cells were harvested and lysed in RIPA buffer on ice for 30 min, followed by centrifugation at 14 000g for 10 min at 4 °C. Samples (40 μg) were loaded and separated by sodium dodecyl sulfate-polyacrylamide gel electrophoresis, transferred to polyvinylidene fluoride membranes, and then blocked with 5% nonfat milk at room temperature for 4 h, followed by incubation with primary antibody in TBST at 4 °C overnight. After extensive washing with TBST (3 times, 10 min), the blots were incubated with the HRP-conjugated secondary antibody for 1 h at room temperature. After washing with TBST (3 times, 10 min), the membranes were visualized using ECL reagents, and images were scanned and quantified using Image Lab software (Bio-Rad Laboratories, Inc., CA, USA). Each band was normalized to the loading control β-actin.

4.9. Statistical Analysis. Experiments were carried out at least in triplicate, and the results were analyzed using GraphPad Prism software version 7 (Graph Pad software Inc., CA, USA) and expressed as the mean ± SD. One-way analysis of variance followed by Tukey's test for multiple comparisons was used to analyze the statistical significance. A p-value < 0.05 was considered statistically significant.

AUTHOR INFORMATION

Corresponding Author

*E-mail: fanpeihong@sdu.edu.cn.

ORCID

Peihong Fan: 0000-0001-5529-8922

Author Contributions

§S.W. and Q.L. contributed equally to this work.

Notes

The authors declare no competing financial interest.

ACKNOWLEDGMENTS

This work was financially supported by the National Natural Science Foundation of China (grant no. 81473323).

ABBREVIATIONS

AD, Alzheimer's disease; AMPK, adenosine monophosphate-activated protein kinase; CLG, coumaroylaminobutanol glucopyranoside; FoxO, Forkhead box O; HO-1, hemeoxygenase-1; IL, interleukin; IKK, IκB kinase; LPS, lipopolysaccharide; MyD88, myeloid differentiation primary response gene 88; NF-κB, nuclear factor-kappa B; NO, nitric oxide; Nrf-2, nuclear factor erythroid 2-related factor 2; PGC-1α, peroxisome proliferator-activated receptor γ co-activator 1α; ROS, reactive oxygen species; SIRT, silent information regulator; TLR4, toll-like receptor 4; TNF-α, tumor necrosis factor-α

REFERENCES

(1) Xu, L.; He, D.; Bai, Y. Microglia-mediated inflammation and neurodegenerative disease. *Mol. Neurobiol.* **2016**, *53*, 6709−6715.

(2) Smith, J. A.; Das, A.; Ray, S. K.; Banik, N. L. Role of pro-inflammatory cytokines released from microglia in neurodegenerative diseases. *Brain Res. Bull.* **2012**, *87*, 10−20.

(3) Callaway, J. C. Hempseed as a nutritional resource: An overview. *Euphytica* **2004**, *140*, 65−72.

(4) Zhou, Y.; Wang, S.; Lou, H.; Fan, P. Chemical constituents of hemp (*Cannabis sativa* L.) seed with potential anti-neuroinflammatory activity. *Phytochem. Lett.* **2018**, *23*, 57−61.

(5) Luo, Q.; Yan, X.; Bobrovskaya, L.; Ji, M.; Yuan, H.; Lou, H.; Fan, P. Anti-neuroinflammatory effects of grossamide from hemp seed via suppression of TLR-4-mediated NF-κB signaling pathways in lipopolysaccharide-stimulated BV2 microglia cells. *Mol. Cell. Biochem.* **2017**, *428*, 129−137.

(6) Yan, X.; Tang, J.; Dos Santos Passos, C.; Nurisso, A.; Simões-Pires, C. A.; Ji, M.; Lou, H.; Fan, P. Characterization of lignanamides from hemp (*Cannabis sativa* L.) seed and their antioxidant and acetylcholinesterase inhibitory activities. *J. Agric. Food Chem.* **2015**, *63*, 10611−10619.

(7) Chen, N. Y.; Liu, C. W.; Lin, W.; Ding, Y.; Bian, Z. y.; Huang, L.; Huang, H.; Yu, K. H.; Chen, S. B.; Sun, Y.; Wei, L.; Peng, J. H.; Pan, S.-L. Extract of fructus cannabis ameliorates learning and memory impairment induced by D-galactose in an aging rats model. *J. Evidence-Based Complementary Altern. Med.* **2017**, *2017*, 1−13.

(8) Luo, J.; Yin, J.; Wu, H.; Wei, Q. Extract from Fructus cannabis activating calcineurin improved learning and memory in mice with chemical drug-induced dysmnesia. *Acta Pharmacol. Sin.* **2003**, *24*, 1137−1142.

(9) Lehnardt, S.; Lachance, C.; Patrizi, S.; Lefebvre, S.; Follett, P. L.; Jensen, F. E.; Rosenberg, P. A.; Volpe, J. J.; Vartanian, T. The toll-like receptor TLR4 is necessary for lipopolysaccharide-induced oligodendrocyte injury in the CNS. *J. Neurosci.* **2002**, *22*, 2478−2486.

(10) Hines, D. J.; Choi, H. B.; Hines, R. M.; Phillips, A. G.; MacVicar, B. A. Prevention of LPS-induced microglia activation, cytokine production and sickness behavior with TLR4 receptor interfering peptides. *PLoS One* **2013**, *8*, No. e60388.

(11) Park, J.; Min, J.-S.; Kim, B.; Chae, U.-B.; Yun, J. W.; Choi, M.-S.; Kong, I.-K.; Chang, K.-T.; Lee, D.-S. Mitochondrial ROS govern the LPS-induced pro-inflammatory response in microglia cells by regulating MAPK and NF-κB pathways. *Neurosci. Lett.* **2015**, *584*, 191−196.

(12) Park, S. Y.; Choi, M. H.; Park, G.; Choi, Y.-W. Petasites japonicus bakkenolide B inhibits lipopolysaccharide-induced pro-inflammatory cytokines via AMPK/Nrf2 induction in microglia. *Int. J. Mol. Med.* **2018**, *41*, 1683−1692.

(13) Salminen, A.; Hyttinen, J. M. T.; Kaarniranta, K. AMP-activated protein kinase inhibits NF-κB signaling and inflammation: impact on healthspan and lifespan. *J. Mol. Med.* **2011**, *89*, 667−676.

(14) Catorce, M. N.; Gevorkian, G. LPS-induced murine neuroinflammation model: main features and suitability for pre-clinical assessment of nutraceuticals. *Curr. Neuropharm.* **2016**, *14*, 155−164.

(15) He, P.; Yan, S.; Zheng, J.; Gao, Y.; Zhang, S.; Liu, Z.; Liu, X.; Xiao, C. Eriodictyol attenuates LPS-induced neuroinflammation, amyloidogenesis, and cognitive impairments via the inhibition of NF-κB in male C57BL/6J mice and BV2 microglial cells. *J. Agric. Food Chem.* **2018**, *66*, 10205−10214.

(16) Beutler, B. Tlr4: central component of the sole mammalian LPS sensor. *Curr. Opin. Immunol.* **2000**, *12*, 20−26.

(17) Lu, Y. C.; Yeh, W. C.; Ohashi, P. S. LPS/TLR4 signal transduction pathway. *Cytokine* **2008**, *42*, 145−151.

(18) Christman, J. W.; Lancaster, L. H.; Blackwell, T. S. Nuclear factor κB: a pivotal role in the systemic inflammatory response

DOI: 10.1021/acsomega.9b02168
ACS Omega 2019, 4, 16517−16523

syndrome and new target for therapy. *Intensive Care Med.* **1998**, *24*, 1131−1138.
(19) Yuan, L.; Wu, Y.; Ren, X.; Liu, Q.; Wang, J.; Liu, X. Isoorientin attenuates lipopolysaccharide-induced pro-inflammatory responses through down-regulation of ROS-related MAPK/NF-κB signaling pathway in BV-2 microglia. *Mol. Cell. Biochem.* **2014**, *386*, 153−165.
(20) Buendia, I.; Michalska, P.; Navarro, E.; Gameiro, I.; Egea, J.; León, R. Nrf2−ARE pathway: An emerging target against oxidative stress and neuroinflammation in neurodegenerative diseases. *Pharmacol. Ther.* **2016**, *157*, 84−104.
(21) Lim, J. L.; Wilhelmus, M. M. M.; de Vries, H. E.; Drukarch, B.; Hoozemans, J. J. M.; van Horssen, J. Antioxidative defense mechanisms controlled by Nrf2: state-of-the-art and clinical perspectives in neurodegenerative diseases. *Arch. Toxicol.* **2014**, *88*, 1773−1786.
(22) Pae, H.-O.; Chung, H.-T. Heme oxygenase-1: its therapeutic roles in inflammatory diseases. *Immune Netw.* **2009**, *9*, 12−19.
(23) Magesh, S.; Chen, Y.; Hu, L. Small molecule modulators of Keap1-Nrf2-ARE pathway as potential preventive and therapeutic agents. *Med. Res. Rev.* **2012**, *32*, 687−726.
(24) Ronnett, G. V.; Ramamurthy, S.; Kleman, A. M.; Landree, L. E.; Aja, S. AMPK in the brain: its roles in energy balance and neuroprotection. *J. Neurochem.* **2009**, *109*, 17−23.
(25) Łabuzek, K.; Liber, S.; Gabryel, B.; Okopień, B. Metformin has adenosine-monophosphate activated protein kinase (AMPK)-independent effects on LPS-stimulated rat primary microglial cultures. *Pharmacol. Rep.* **2010**, *62*, 827−848.
(26) Velagapudi, R.; El-Bakoush, A.; Lepiarz, I.; Ogunrinade, F.; Olajide, O. A. AMPK and SIRT1 activation contribute to inhibition of neuroinflammation by thymoquinone in BV2 microglia. *Mol. Cell. Biochem.* **2017**, *435*, 149−162.
(27) Chen, H.; Sohn, J.; Zhang, L.; Tian, J.; Chen, S.; Bjeldanes, L. F. Anti-inflammatory effects of chicanine on murine macrophage by down-regulating LPS-induced inflammatory cytokines in IκBα/MAPK/ERK signaling pathways. *Eur. J. Pharmacol.* **2014**, *724*, 168−174.
(28) Harikrishnan, H.; Jantan, I.; Haque, M. A.; Kumolosasi, E. Anti-inflammatory effects of Phyllanthus amarus Schum. & Thonn. through inhibition of NF-κB, MAPK, and PI3K-Akt signaling pathways in LPS-induced human macrophages. *BMC Complementary Altern. Med.* **2018**, *18*, 224.

DOI: 10.1021/acsomega.9b02168
ACS Omega 2019, 4, 16517−16523